All-fiber terahertz time-domain spectrometer operating at 1.5 µm telecom wavelengths

B. Sartorius*, H. Roehle, H. Künzel, J. Böttcher, M. Schlak, D. Stanze, H. Venghaus, and M. Schell

Fraunhofer Institute for Telecommunications, Heinrich-Hertz-Institut, Einsteinufer 37, 10587 Berlin, Germany
**Corresponding author: bernd.sartorius@hhi.fraunhofer.de*

Abstract: The worldwide first all-fiber THz time-domain spectrometer for operation at 1.5 µm is presented. Applications up to 3 THz are demonstrated. Key devices are photoconductive antennas based on novel LT InGaAs/InAlAs multi-layer structures.

OCIS codes: (300.6495) Spectroscopy, terahertz; (120.4290) Nondestructive testing.

References and links

1. B. S. Gupta, J. F. Whitaker, and G. A. Mourou, "Ultrafast carrier dynamics in III-V semiconductors grown by molecular-beam epitaxy at very low substrate temperatures," IEEE J. Quantum Electron. **28,** 2464 (1992)
2. D. Mittleman, ed., "Terahertz Imaging," in *Sensing with Terahertz Radiation,* ISBN 3-540-43110-1 (Springer Verlag, Berlin-Heidelberg, New York, 2003), pp. 117-153.
3. I. Duling and D. Zimdars, "Compact TD-THz systems offer flexible, turnkey imaging solutions," Laser Focus World, April 2007
4. M. Suzuki and M. Tonouchi, "Fe-implanted InGaAs THz emitters for 1.56 µm wavelength excitation," Appl. Phys. Lett. **86**, 051104 (2005)
5. M. Suzuki and M. Tonouchi, "Fe-implanted InGaAs photoconductive terahertz detectors triggered by 1.56 µm femtosecond optical pulses," Appl. Phys. Lett. **86**, 163504 (2005)
6. N. Chimot, J. Mangeney, L. Joulaud, P. Crozat, H. Bernas, K. Blary, and J. F. Lampin, "Terahertz radiation from heavy-ion-irradiated $In_{0.53}Ga_{0.47}As$ photoconductive antenna excited at 1.55 µm," Appl. Phys. Lett. **87**, 193510 (2005)
7. H. Künzel, J. Böttcher, R. Gibis, and G. Urmann, "Material properties of $In_{0.53}Ga_{0.47}As$ on InP by low-Temperature Molecular Beam Epitaxy," Appl. Phys. Lett. **61**, 1347 (1992)
8. R. Wilk, M. Mikulics, K. Biermann, H. Künzel, I. Z. Kozma, R. Holzwarth, B. Sartorius, M. Mei, and M. Koch, "THz time-domain spectrometer based on LT-InGaAs photoconductive antennas exited by a 1.55 µm fibre laser," paper CThR2 on Conference on Lasers and Electro-Optics 2007, Baltimore, Maryland, USA, May 6-11, 2007

1. Introduction

State-of-the-art optical THz systems typically deploy Ti:Sapphire short pulse lasers at 800 nm, low temperature (< 200 °C) MBE grown LT GaAs photoconductive antennas, and free space optics [1,2]. Our target is the development of a fiber based system operating at the telecom wavelength 1.5 µm. Expected advantages are firstly the lower cost, higher stability and reduced size of pulsed fiber lasers as compared to the conventional Ti:Sapphire lasers. Secondly, a lot of versatile, mature and low cost fiber and semiconductor components are available in the 1.5 µm range thanks to the many years of development in fiber-based telecom components. Thirdly, as a consequence, handheld THz systems can be set up, using fixed optoelectronic control boxes and fiber connected movable THz emitter and coherent receiver heads (Fig. 1). The new Picometrix T-Ray 4000 TD-THz System [3] can here be taken as an example which, however, has still to be operated at short wavelengths ($\leq$ 800 nm) due to the conventionally available LT GaAs photoconductive antennas. The key components for our proposed system thus are ultrafast photoconductive antennas which are sensitive in the 1.5 µm wavelength range. Up to now, 1.5 µm photoconductors have not been available yet in a

#94776 - $15.00 USD Received 7 Apr 2008; revised 9 May 2008; accepted 9 May 2008; published 13 Jun 2008

quality comparable to LT GaAs. In chapter 2 we describe the development of a novel material matching the demands for 1.5 µm THz applications. The assembly of an all-fiber time-domain spectrometer is described in chapter 3, its performance and first applications in chapter 4.

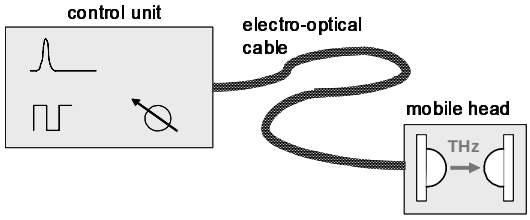

Fig. 1. Scheme of fiber based optical THz system

2. THz photoconductors for 1.5 µm operation

Our material of choice for 1.5 µm photoconductors is InGaAs grown lattice-matched on InP substrates using MBE. Low temperature growth ($T_g < 200$ °C) of InGaAs, similar to LT GaAs, was performed using an As_4 beam. In correspondence with the decreasing As_4 desorption rate with decreasing T_g the V/III ratio was kept konstant at a value of 2 by reducing the beam equivalent pressure ratio from 15 at 500 °C to 9 at 100 °C. As for the case of LT GaAs on GaAs, formation of native defects as a consequence of excess As incorporation occurs, most probably As_{Ga} anitsites leading to the mandatory ultrafast recombination and photo response. However, quite different to LT GaAs, which has a very high dark resistivity, the InGaAs becomes highly conductive in the LT growth mode.

With decrease of the growth temperature the carrier concentration increases by orders of magnitude, as is shown in Fig. 2. The resulting high dark conductivity is not acceptable for THz photoconductive antennas. Due to this well known effect, alternative techniques have been developed to simultaneously achieve high resistivity and ultrafast behavior of InGaAs. Fe doping of MOVPE grown layers [4,5] as well as heavy ion bombardment [6] have both been applied, but without achieving material characteristics equivalent to LT GaAs. We thus decided to go back to low temperature growth of InGaAs and to develop means for increasing the resistivity of this material.

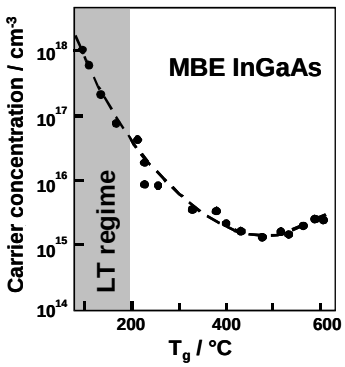

Fig. 2. Carrier concentration of LT InGaAs

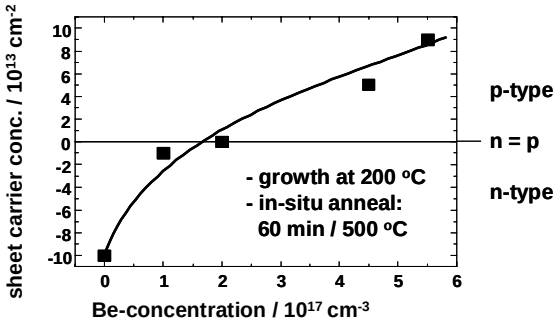

Fig. 3. Be doping and carrier concentration

The first modification we apply is compensating the free electron concentration by doping with an acceptor matched to the individual growth temperature. Beryllium is chosen, and Fig. 3 shows the carrier concentration of InGaAs grown at low temperatures versus the Be doping level [7]. Additional in-situ annealing using the conditions given in Fig. 3 supports Be

#94776 - $15.00 USD Received 7 Apr 2008; revised 9 May 2008; accepted 9 May 2008; published 13 Jun 2008

incorporation at Ga sites at the expense of As_{Ga} anitsite formation. The significant reduction of the free carrier concentration can clearly be noticed. However, a perfect balancing of the Be doping and the background carrier concentration is required which is extremely difficult to adjust. Additional means seemed to be very helpful to relax this situation.

Therefore, a second development step we introduced towards treating this target is embedding of the photoconductive InGaAs material between InAlAs layers (Fig. 4(a)) grown at the same conditions, e.g. low T_g and V/III ratio. This material has a higher bandgap (1.46 eV), it is transparent at 1.5 µm and does not contribute to the photoconductivity. It further exhibits a high resistivity and therefore does not deteriorate the dark current. The essential feature of the InAlAs is the high concentration of deep electron traps. Electrons can be captured out of the InGaAs photoconductive layer via tunneling processes and are trapped within the InAlAs (Fig. 4(b)). The dark resistivity of the InGaAs can be increased in this way. However, the trapping effect works only for rather thin photoconductive layers in the 10…15 nm range, where the distance between the electrons and the trapping centers is short to facilitate a high amount of tunneling processes. Nevertheless, the InGaAs thickness chosen leads to only a minor shift of the effective band gap towards 1.55 µm due to quantization effects. This was controlled by measuring the absorption spectrum at the fundamental effective gap. A relatively soft staircase-type onset of absorption without any excitonic resonances close to 0.8 eV was deduced. Unfortunately, in such a thin layer the absorption of light is very low and photoconductive antennas made from this material are very inefficient. Multilayer structures of alternating photoconductive and trapping layers are a way for improving the amount of absorbed light. In our final structure we have grown 100 periods of 12 nm thick InGaAs layers (lattice-matched to InP) between 8 nm InAlAs spacers, resulting in a photoconductor with an integral thickness of 1.2 µm (Fig. 4(c)).

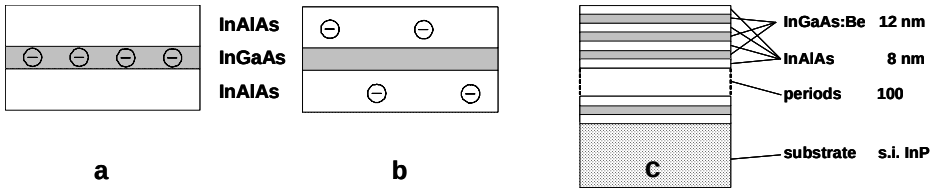

Fig. 4. (a). embedded photoconductor; (b). electron trapping; (c). multilayer structure

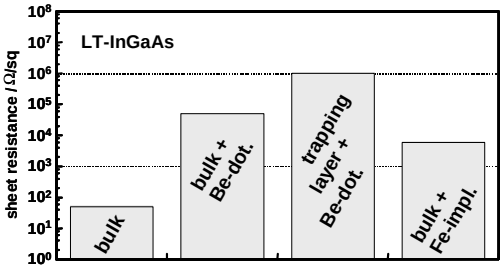

Fig. 5. Resistivity of differently processed InGaAs

The resistivities achieved by simultaneous Be doping and introduction of the trapping layers are shown in Fig. 5. For comparison the value for MOVPE grown InGaAs:Fe is also given as a reference. Our newly developed structures result in a resistivity increased by four orders of magnitude, which is markedly above the values obtained for InGaAs:Fe. Thus, the developed novel heterostructures appear well suited for THz applications. Planar antennas (bow-tie, dipole and strip-line type) were processed on the basis of the material described. First evaluations were performed in an existing free-space 800 nm test bed. A performance at least similar to LT GaAs was found by replacing the existing LT GaAs by the newly

#94776 - $15.00 USD Received 7 Apr 2008; revised 9 May 2008; accepted 9 May 2008; published 13 Jun 2008

developed photoconductive elements [8]. That was treated as a good starting point for developing a completely fiber-coupled THz time-domain spectrometer for 1.5 µm operation.

3. All-fiber THz time domain spectrometer

In a first step the developed THz photoconductive antennas had to be packaged into fiber-coupled modules. Figure 6 shows a photograph of the developed housing. On the left one can see the optical fiber input, and on the right the Si lens where the THz radiation is emitted. Chips of 4x4 mm^2 standard size can be inserted and exchanged, while gold contacts ensure electrical connection without need for bonding processes. The fiber can be positioned to the conductive gap using built-in adjustment screws. These fiber-coupled and movable THz emitter and detector heads are key elements for the all-fiber THz system sketched in Fig. 1.

Fig. 6. Emitter module

The scheme of the complete all-fiber time domain spectrometer is shown in Fig. 7. A pulsed fiber laser from Menlo Systems is used. The laser emits at 1550 nm, delivers 100 fs pulses, and operates at 100 MHz repetition rate. Two fiber outputs with up to 100 mW mean power each can be used for driving the emitter with a strip-line antenna (width 100 µm) inside and the receiver with a 90 degree bow-tie antenna (gap 10 µm). A programmable fiber delay line (JDS-Fitel HD4) is inserted between laser and receiver in order to sample the received pulse voltage. The bias at the emitter (5…25 V) is modulated at 3 kHz, and the photocurrent of the receiver is detected using a lock-in amplifier synchronized to the bias modulation. Normally a compartment covering the THz radiation path is used, which allows purging this area with dry nitrogen in order to avoid water vapor absorption.

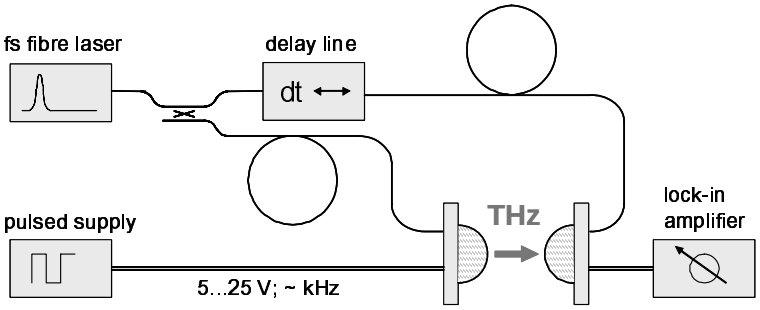

Fig. 7. Scheme of spectrometer system

For the design of the fiber circuitry one has to take into account the broad spectrum according to the 100 fs pulses (~ 100 nm) and the dispersion of the fiber. The short pulses are needed not at the output of the laser but in front of the excited antennas. Menlo Systems thus has incorporated a fixed pre-compensation for about 10 m fiber inside of their laser unit. Fine adjustment of the external fiber length has been done using autocorrelation measurements. The trace of the autocorrelator (APE Pulse Check) after length optimization is shown in Fig. 8. A pulse width as short as < 100 fs is achieved. Such pulses excite the fiber-coupled

#94776 - $15.00 USD Received 7 Apr 2008; revised 9 May 2008; accepted 9 May 2008; published 13 Jun 2008

emitter and receiver antennas in the developed time-domain spectrometer. The achieved performance of the complete 1.5 µm fiber system is described in the following.

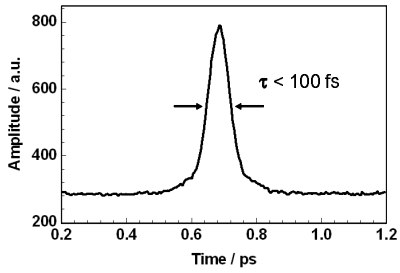

Fig. 8. Autocorrelator trace after 10 m SMF, at the antenna position

4. System performance and demonstration of typical applications

The system performance has been evaluated with the THz path purged with dry nitrogen. The detected pulse trace versus time delay is shown in Fig. 9(a). The sharp pulse with a width of 750 fs indicates the high speed of the developed InGaAs/InAlAs photoconductive switches. This can be recognized also in the according Fourier transform spectrum (Fig. 9(b)). The detectable frequencies extend up to 3 THz; the noise floor allows high quality spectral measurements up to 2 THz.

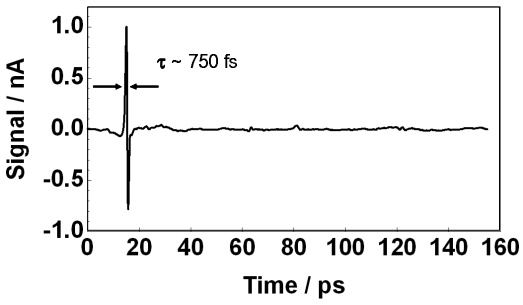

Fig. 9. (a). Pulse trace under nitrogen purging;

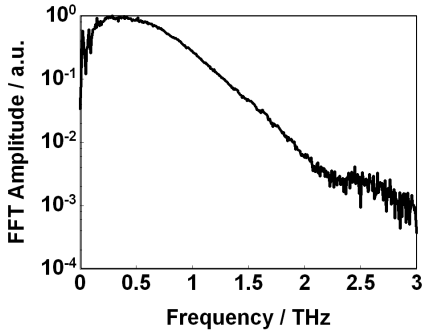

(b). Fourier spectrum, extending up to 3 THz

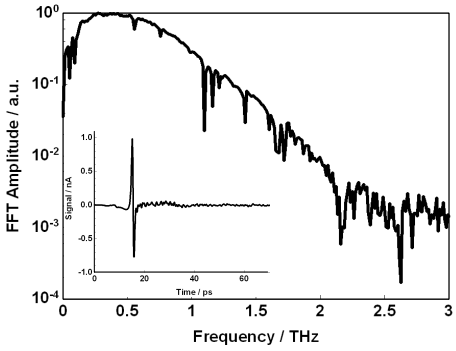

Fig. 10. (a). Pulse and FFT without nitrogen purging;

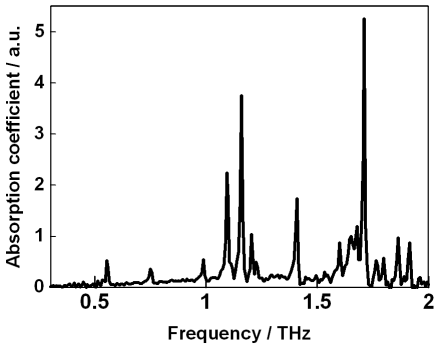

(b). associated absorption spectrum

#94776 - $15.00 USD Received 7 Apr 2008; revised 9 May 2008; accepted 9 May 2008; published 13 Jun 2008

Figure 10 gives an example for spectroscopic applications. The THz beam in the case of Fig. 10(a) has not been purged with nitrogen, and thus the absorption of water vapor in air affects the THz waves and the Fourier transform spectrum. The absorption can be calculated by dividing the spectra without and with water vapor. Figure 10(b) shows as the result a spectrum in which the well known absorption lines of water vapor are clearly resolved. The example demonstrates an excellent spectroscopic performance up to at least 2 THz.

All the pulse traces shown in this report are recorded with the following settings: transmitter voltage 25 V, average optical power at transmitter 10 mW, at receiver 6 mW, lock-in integration time 30 ms, 8 times averaging of each reading, delay-line step-size 50 fs.

Another type of THz applications regards the inspection of materials in closed boxes. The example we give here is the investigation of InP substrates in Fluoroware boxes (insert in Fig. 11). Figure 11 shows as reference the THz beam in air (dotted trace) and with an empty box in the THz beam (full black trace). The box is transparent for THz. Its refractive index difference to air generates a delay of a few ps. Next, a box with a semi-insulating substrate inside is inspected. The substrate is transparent, but the THz pulse is additionally delayed (dark grey trace). Measuring this additional delay and knowing the index of refraction of InP one can calculate the thickness of the wafer (400 µm) in the closed box. At last, a box with another substrate inside is inspected and complete blocking of the THz radiation is found (light grey trace). Thus one can conclude the substrate is conductive, in our case it is InP:Sn. Differently doped substrates can thus be identified in the closed box using the THz inspection method.

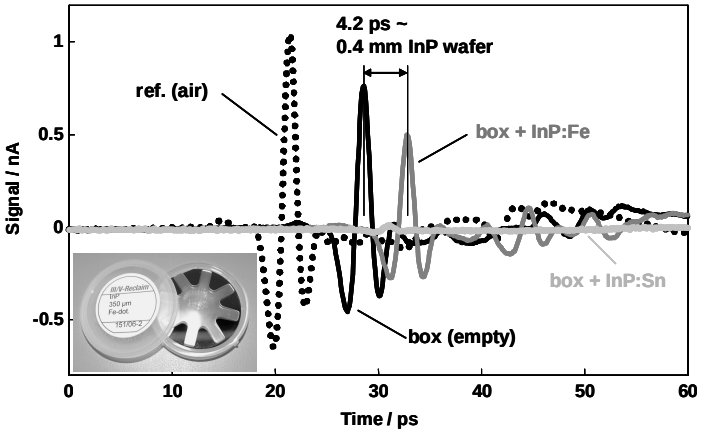

Fig. 11. THz through box

5. Summary and outlook

The worldwide first all-fiber Terahertz time-domain spectrometer for operation at the telecom wavelength 1.5 µm has been presented. The enabling key devices are photoconductive antennas based on novel LT InGaAs/InAlAs multi-layer structures. Ultrafast photo response at 1.5 µm and high dark resistivity are achieved with this material. Planar THz antennas have been integrated and fiber-coupled THz emitter and receiver heads with Si lenses have been assembled. A 1.5 µm pulsed fiber-ring laser of Menlo Systems with built-in pre-compensation is used as source. Optimizing the fiber length a pulse width of < 100 fs could be achieved at the fiber output in front of the antenna. The THz spectrum covered by the system extends up to 3 THz. Two applications have been demonstrated, a spectroscopic one and material inspection through a closed box. The novel ultrafast photoconductive switches operating at 1.5 µm wavelengths open the way for exploiting versatile and low-cost telecom and fiber components for application in movable and handheld THz TDS systems.

#94776 - $15.00 USD Received 7 Apr 2008; revised 9 May 2008; accepted 9 May 2008; published 13 Jun 2008